Titre: Title:	Diffusion magnetic resonance imaging reveals tract-specific microstructural correlates of electrophysiological impairments in non-myelopathic and myelopathic spinal cord compression
Auteurs: Authors:	Jan Valošek, René Labounek, Tomáš Horák, Magda Horáková, Petr Bednařík, Miloš Keřkovský, Jan Kočica, Tomáš Rohan, Christophe Lenglet, Julien Cohen-Adad, Petr Hluštík, Eva Vlčková, Zdeněk Kadaňka, Josef Bednařík, & Alena Svatkova
Date:	2021
Type:	Article de revue / Article
Référence: Citation:	Valošek, J., Labounek, R., Horák, T., Horáková, M., Bednařík, P., Keřkovský, M., Kočica, J., Rohan, T., Lenglet, C., Cohen-Adad, J., Hluštík, P., Vlčková, E., Kadaňka, Z., Bednařík, J., & Svatkova, A. (2021). Diffusion magnetic resonance imaging reveals tract-specific microstructural correlates of electrophysiological impairments in non-myelopathic and myelopathic spinal cord compression. European Journal of Neurology, 28(11), 3784-3797. https://doi.org/10.1111/ene.15027

Titre de la revue: Journal Title:	European Journal of Neurology (vol. 28, no. 11)
Maison d'édition: Publisher:	John Wiley & Sons
URL officiel: Official URL:	https://doi.org/10.1111/ene.15027
Mention légale: Legal notice:	

Received: 15 June 2021 | Accepted: 16 July 2021

DOI: 10.1111/ene.15027

european journal of neurology
the official journal of the european academy of neurology

ORIGINAL ARTICLE

Diffusion magnetic resonance imaging reveals tract-specific microstructural correlates of electrophysiological impairments in non-myelopathic and myelopathic spinal cord compression

Jan Valošek[1,2] | René Labounek[1,3] | Tomáš Horák[4,5,6] | Magda Horáková[5,6] | Petr Bednařík[4,7] | Miloš Keřkovský[6,8] | Jan Kočica[5,6] | Tomáš Rohan[6,8] | Christophe Lenglet[9] | Julien Cohen-Adad[10,11,12] | Petr Hluštík[1] | Eva Vlčková[5,6] | Zdeněk Kadaňka Jr.[5,6] | Josef Bednařík[4,5,6] | Alena Svatkova[4,13]

[1]Department of Neurology, Faculty of Medicine and Dentistry, Palacký University, Olomouc, Czechia

[2]Department of Biomedical Engineering, University Hospital, Olomouc, Czechia

[3]Division of Clinical Behavioral Neuroscience, Department of Pediatrics, University of Minnesota, Minneapolis, Minnesota, USA

[4]Central European Institute of Technology, Masaryk University, Brno, Czechia

[5]Department of Neurology, University Hospital Brno, Brno, Czechia

[6]Faculty of Medicine, Masaryk University, Brno, Czechia

[7]High Field MR Centre, Department of Biomedical Imaging and Image-guided Therapy, Medical University of Vienna, Vienna, Austria

[8]Department of Radiology and Nuclear Medicine, University Hospital Brno, Brno, Czechia

[9]Center for Magnetic Resonance Research, Department of Radiology, University of Minnesota, Minneapolis, Minnesota, USA

[10]NeuroPoly Lab, Institute of Biomedical Engineering, Polytechnique Montreal, Montreal, Quebec, Canada

[11]Functional Neuroimaging Unit, CRIUGM, University of Montreal, Montreal, Quebec, Canada

[12]Mila - Quebec AI Institute, Montreal, Quebec, Canada

[13]Department of Medicine III, Clinical Division of Endocrinology and Metabolism, Medical University of Vienna, Vienna, Austria

Correspondence
Alena Svatkova, Department of Medicine III, Clinical Division of Endocrinology and Metabolism, Medical University of Vienna, Vienna, Austria.
Email: alena.svatkova@meduniwien.ac.at

Funding information
The core facility Multimodal and Functional Imaging Laboratory, Masaryk University, CEITEC, supported by the MEYS CR (LM2018129 Czech-BioImaging) is acknowledged. This research is funded by the Czech Health Research Council grants NV18-04-00159 and by the Ministry of Health of the Czech Republic project for conceptual development in research organizations, ref. 65269705 (University Hospital, Brno, Czech Republic). JV has received "Aktion Österreich-Tschechien, AÖCZ-Semesterstipendien" scholarship MPC-

Abstract

Background and purpose: Non-myelopathic degenerative cervical spinal cord compression (NMDC) frequently occurs throughout aging and may progress to potentially irreversible degenerative cervical myelopathy (DCM). Whereas standard clinical magnetic resonance imaging (MRI) and electrophysiological measures assess compression severity and neurological dysfunction, respectively, underlying microstructural deficits still have to be established in NMDC and DCM patients. The study aims to establish tract-specific diffusion MRI markers of electrophysiological deficits to predict the progression of asymptomatic NMDC to symptomatic DCM.

Methods: High-resolution 3 T diffusion MRI was acquired for 103 NMDC and 21 DCM patients compared to 60 healthy controls to reveal diffusion alterations and relationships between tract-specific diffusion metrics and corresponding electrophysiological measures and compression severity. Relationship between the degree of DCM disability, assessed by the modified Japanese Orthopaedic Association scale, and tract-specific microstructural changes in DCM patients was also explored.

2020-00013 from Austrian Agency for International Cooperation in Education and Research (OeAD-GmbH), Mobility Programmes, Bilateral and Multilateral Cooperation (MPC) financed by Federal Ministry of Education, Science and Research (BMBWF) of Austria. AS has received funding from the European Union's Horizon 2020 research and innovation programme under the Marie Skłodowska-Curie grant agreement no. 794986. PB was partially supported by a NARSAD Young Investigator Grant from the Brain and Behavior Research Foundation (grant no. 27238) and by the European Union's Horizon 2020 research and innovation programme under the Marie Skłodowska-Curie grant agreement no. 846793. CL is partly supported by NIH grants P41 EB027061 and P30 NS076408. Computational resources were supplied by the project "e-Infrastruktura CZ" (e-INFRA LM2018140) provided within the program Projects of Large Research, Development and Innovations Infrastructures. JCA is funded by the Canada Research Chair in Quantitative Magnetic Resonance Imaging (950-230815), the Canadian Institute of Health Research (CIHR FDN-143263), the Canada Foundation for Innovation (32454, 34824), the Fonds de Recherche du Québec—Santé (28826), the Natural Sciences and Engineering Research Council of Canada (RGPIN-2019-07244), the Canada First Research Excellence Fund (IVADO and TransMedTech), the Courtois NeuroMod project and the Quebec BioImaging Network (5886, 35450).

Results: The study identified diffusion-derived abnormalities in the gray matter, dorsal and lateral tracts congruent with trans-synaptic degeneration and demyelination in chronic degenerative spinal cord compression with more profound alterations in DCM than NMDC. Diffusion metrics were affected in the C3-6 area as well as above the compression level at C3 with more profound rostral deficits in DCM than NMDC. Alterations in lateral motor and dorsal sensory tracts correlated with motor and sensory evoked potentials, respectively, whereas electromyography outcomes corresponded with gray matter microstructure. DCM disability corresponded with microstructure alteration in lateral columns.

Conclusions: Outcomes imply the necessity of high-resolution tract-specific diffusion MRI for monitoring degenerative spinal pathology in longitudinal studies.

KEYWORDS
diffusion magnetic resonance imaging, diffusion tensor imaging, spinal cord compression

INTRODUCTION

The relative resilience of the cervical spinal cord (CSC) to degenerative changes might delay the development of clinically manifest myelopathy and result in non-myelopathic degenerative cervical spinal cord compression (NMDC) [1,2]. The prevalence of NMDC progressively increases throughout aging affecting up to 40% of Caucasian individuals over 60 years of age [3-5]. Over time, a portion of NMDC patients progress into potentially irreversible degenerative cervical myelopathy (DCM) [2,6], which is the most common non-traumatic cause of CSC dysfunction. Delineation of risk factors of NMDC progression to the DCM remains an unsolved challenge [2,6,7]. Whilst radiological measures such as cross-sectional area (CSA), anteroposterior diameter or compression ratio (CR) together with electrophysiological abnormalities might be useful in predicting DCM development [6], standard clinical magnetic resonance imaging (MRI) protocols fail to describe microstructural CSC abnormalities in NMDC and DCM. Hyperintensity on T_2-weighted scans, considered as a radiological correlate of myelopathy, is not inevitably observed even in the most severe DCM patients with clinical myelopathic signs [8]. Yet, it remains a critical factor influencing decision-making in decompressive surgery [9]. Thus, quantitative MRI markers are urgently needed to detect early microstructural NMDC changes and predict progression into symptomatic DCM.

Whereas previous studies demonstrated the ability of diffusion MRI (dMRI) to depict profound microstructural CSC alteration in DCM patients [10-15], NMDC reports provided inconclusive outcomes [6,16-18]. However, all previous studies utilized single-shell dMRI protocols that limited estimation of the high-order diffusion models and exclusively quantified the diffusion tensor imaging (DTI) model [19]. Whereas DTI metrics are sensitive to microstructural integrity (i.e., fractional anisotropy [FA]) and axonal, myelin or membrane density deficits (i.e., axial [AD], radial [RD] and mean diffusivity [MD], respectively), the single tensor per voxel does not account for axonal, glial and extracellular compartments within the tissue and remains nonspecific [20]. To address this issue, optimized multi-shell high angular resolution diffusion imaging (HARDI) sequence with reduced field of view, so-called HARDI-ZOOMit [21], were utilized to estimate critical microstructural information from single-compartment DTI and the more advanced multi-compartment ball-and-sticks model [22]. The ball-and-sticks model indeed better fits dMRI data than DTI [20] and more reliably captures the microstructural tissue property in each voxel.

High-resolution multi-shell diffusion and anatomical sequences were combined with state-of-the-art postprocessing [23-26] to achieve selective tract-specific CSC analyses. Capability of the microstructural dMRI metrics to reliably reflect histopathological studies, which previously demonstrated tract-specific distinctions in CSC integrity in degenerative compression [1,27] was also investigated.

Thus, tract-specific alterations in degenerative spinal cord compression at the compression level and also above the compression were hypothesized with more severe deficits in DCM patients than NMDC patients. Relationships between tract-specific dMRI metrics and corresponding electrophysiology and compression severity, previously confirmed as risk factors of DCM development [6] were further hypothesized. Relationship between the degree of DCM disability assessed by the modified Japanese Orthopaedic Association (mJOA) scale [28] and tract-specific diffusion-informed microstructure was also explored.

MATERIALS AND METHODS

Participants

The ethical committee approved the study, and all participants signed an informed consent form. Healthy controls (HC) between 40 and 80 years of age had to be physically healthy with no history of any neurological or other somatic disorder. DCM and NMDC patients were recruited from the database of a spinal center of a tertiary university hospital. The requirements on subjects are shown in Figure 1a.

All subjects underwent a neurological examination to rule out DCM symptoms/signs in HC and NMDC individuals. The degree of DCM disability was assessed by an mJOA scale [28]. All participants underwent standard clinical MRI on a 1.5 T scanner to evaluate radiological signs of degenerative compression and estimate the maximal compression level (MCL), CSA and CR (see Supplementary Materials and Methods).

Non-myelopathic degenerative cervical spinal cord compression patients and DCM patients underwent electrophysiological examination performed by experienced neurologists to detect abnormalities of dorsal columns and/or dorsal gray matter (GM) horns (i.e., somatosensory evoked potentials, SEP), dysfunction in lateral columns (i.e., motor evoked potentials, MEP) and lesions of ventral GM horns (i.e., electromyography, EMG) as described previously [2,29]. Three DCM and 13 NMDC patients did not agree with electrophysiological examination. A detailed description of electrophysiological measures as well as the definition of MEP, SEP and EMG abnormalities is provided in the Supplementary Materials and Methods.

Magnetic resonance imaging acquisition

All participants were scanned on a 3 T Siemens Prisma scanner (Siemens Healthcare, Erlangen, Germany) using 64-channel head/neck and 32-channel spine coils. Lordosis, which could introduce a partial volume effect from the surrounding cerebrospinal fluid and negatively influence field homogeneity, was minimized by keeping the spinal cord as straight as possible. An optimized multi-shell diffusion protocol with reduced field of view [21] with total acquisition time (TA) of 12 min, 46 s covering C3-6 levels with 21 gradient waveform directions with $b_1 = 550$ s/mm^2, 42 directions with $b_2 = 1000$ s/mm^2 and seven b_0 images with anterior–posterior phase encoding, voxel size 0.65 × 0.65 × 3 mm^3 after interpolation in

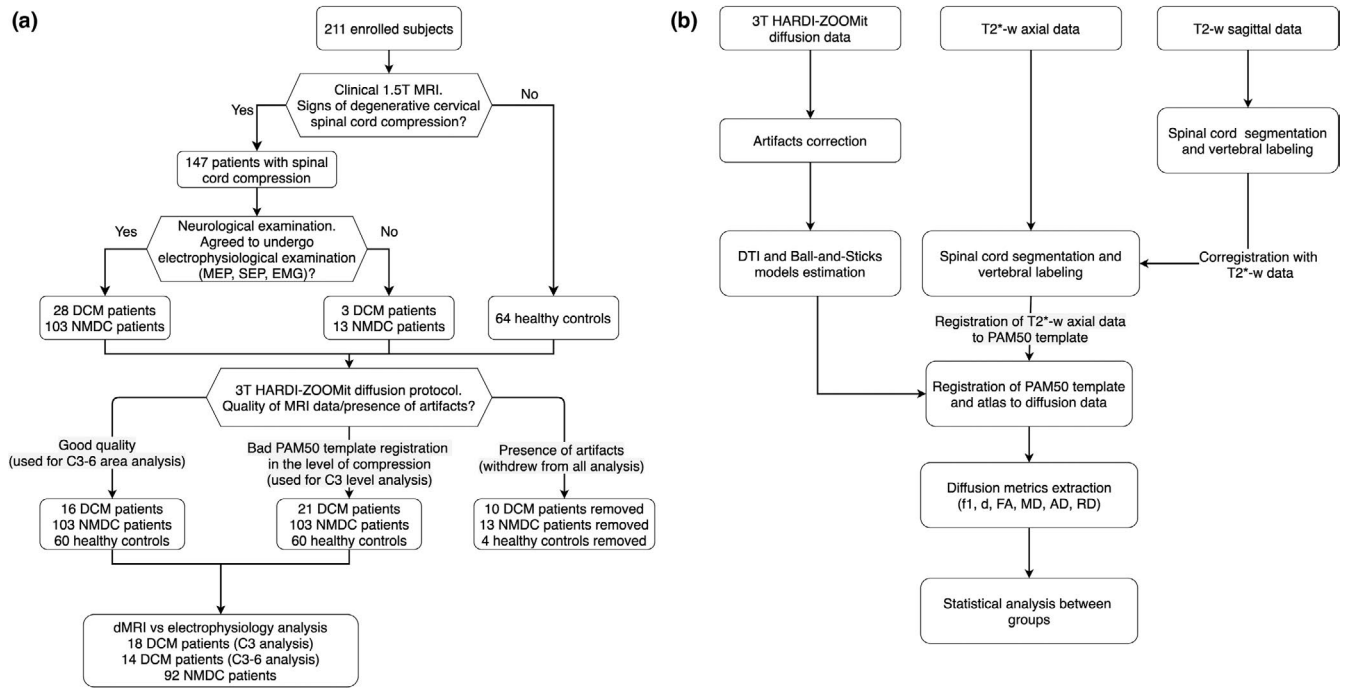

FIGURE 1 Flowcharts of (a) participants' requirements and (b) MRI data analysis

Fourier space, original voxel size 1.30 × 1.30 × 3.00 mm^3 was acquired. An additional five b_0 images with reversed posterior–anterior phase encoding were collected. All gradient waveforms were uniformly sampled over a *q*-space sphere [30]. Axial T_2*-weighted MEDIC images with high grey/white matter contrast using interleaved acquisition (voxel size 0.35 × 0.35 × 2.5 mm^3 after interpolation in Fourier space, original voxel size 0.70 × 0.70 × 2.5 mm^3, TA ≈ 8 min) and T_2-weighted sagittal turbo spin-echo images (voxel size 0.28 × 0.28 × 1.3 mm^3 after interpolation in Fourier space, original voxel size 0.56 × 0.56 × 1.3 mm^3, TA ≈ 9 min) were also collected. Detailed sequence parameters are listed in the Supplementary Materials and Methods.

Image analysis

Images were visually inspected by two independent observers to ensure data quality. Data were analyzed using the Spinal Cord Toolbox [26] v3.2.3 and FMRIB Software Library [31] v5.0.10 (Figure 1b). T_2*-w and T_2-w data were corrected for MR field induced intensity non-uniformities using the N4 bias-field correction tool, and interleaved T_2*-w axial data were additionally slice-by-slice corrected utilizing affine registration between even and odd slices followed by additive image fusion. Spinal cord segmentation and vertebral labeling of T_2-w sagittal data was performed and co-registered with T_2*-w axial data. Then spinal cord segmentation using convolution neural network [23] of T_2*-w axial was performed and vertebral levels were defined [32] using initial information from T_2-w sagittal labeling. Finally, the T_2*-w spinal cord was registered to the PAM50 template [24] using C3 and C6 as labels. Diffusion data were corrected for motion, susceptibility and eddy current artifacts. A conventional DTI [19] model and a multi-compartment ball-and-sticks [22] model were estimated to extract FA, MD, AD and RD as well as f_1 and *d* metrics. The PAM50 template was registered to diffusion data using the initial transformation from the T_2*-w axial image, and the probabilistic spinal cord atlas [25] was warped into diffusion data.

Metric extractions

Diffusion metrics were extracted per subject from all regions of interest (ROIs) utilizing the *sct_extract_metric* function [26] with use of the *maximum a posteriori* optimizing approach [25,26] to eliminate partial volume effect and variability in tract size. ROIs included the GM, ventral, lateral, dorsal columns, fasciculus gracilis, fasciculus cuneatus, lateral corticospinal tracts, spinal lemniscus (i.e., spinothalamic and spinoreticular tracts), dorsal GM horns and ventral GM horns (Figure 2a). Diffusion metrics for individual ROIs were averaged from the whole C3-6 area and from C3 above the compression vertebral level (Figure 2d).

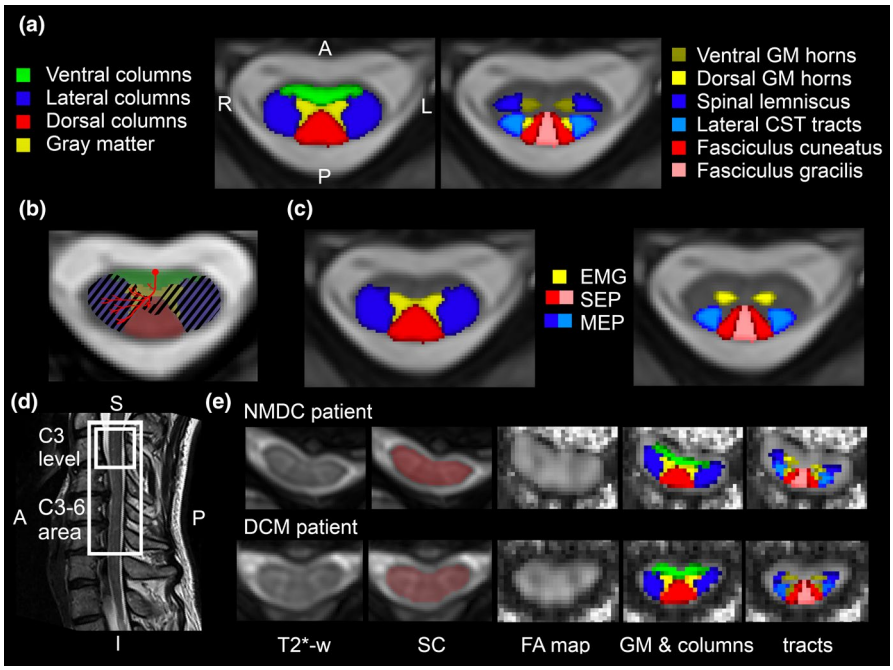

FIGURE 2 (a) Individual ROIs masks from probabilistic PAM50 atlas. (b) Lesion distribution caused by compressed anterior spinal artery. Filled areas are affected by the compression, that is, lateral columns, anterior part of dorsal columns and ventral GM horns. Adapted from Mair and Druckman [27]. (c) Individual ROIs related to electrophysiological measures: EMG, electromyography; SEP, somatosensory evoked potentials; MEP, motor evoked potentials. (d) Two analyzed areas, the C3-6 area and C3 above the compression level. (e) Representative slices from the C4/5 disc from NMDC and DCM patients. From the left: T2*-w axial image, CSC segmentation used for PAM50 registration, fractional anisotropy (FA) map, white matter columns, and gray matter (GM) and individual tracts registered into an FA map

Mean CSA at the C3 level was calculated to quantify atrophy above the compression level from high-resolution T_2*-w data using the *sct_process_segmentation* function [26].

Statistical analysis

Statistical analysis was performed using Matlab R2019b (The Mathworks Inc.), Python 3.7 and SPSS 25 (IBM). Data normality was examined using the Shapiro–Wilk test. Comparison between groups in age, height, weight, body mass index (BMI) and CSA at C3 were tested by the Kruskal–Wallis *H* test, and sex by Fisher's exact test.

Between-group differences in dMRI metrics from the C3-6 area and above the compression (i.e., C3) level were analyzed per individual tract and column using ANCOVA with age and BMI as covariates using Tukey–Kramer post hoc tests. Analyses were corrected using the Holm–Bonferroni correction.

Associations between dMRI metrics from the C3-6 area, age and BMI in 60 controls as well as between CSA and CR at MCL and dMRI metrics from the C3-6 area and C3 above the compression level in DCM and NMDC together with the relationship between the degree of myelopathy (mJOA scale) and dMRI metrics at C3 in DCM were examined using the Spearman correlation. Relationships between electrophysiological abnormalities, reported as categorical and dMRI metrics, were quantified in NMDC and DCM patients by the Mann–Whitney rank tests with Holm–Bonferroni correction. MEPs were related to dMRI from motor tracts, that is, lateral columns and lateral corticospinal tracts. SEPs were correlated with sensory tracts, that is, the dorsal column, fasciculus cuneatus, fasciculus gracilis and dorsal GM horns. Relationships between EMG and dMRI from GM and ventral GM horns (Figure 2c) were examined. Finally, post hoc correlation analysis between quantitative electrophysiological parameters and dMRI metrics was performed (see the Supplementary Materials and Methods).

RESULTS

Participant characteristics

A total of 116 NMDC patients, 31 DCM patients and 64 HC were enrolled in the study. Ten DCM, 13 NMDC patients and four HC were initially excluded due to the presence of motion artifacts, low CSC/cerebrospinal fluid contrast in T2*-w axial images preventing proper CSC segmentation, sub-optimal fat saturation, and dMRI signal dropouts caused by excessive cardiac pulsatile motion.

The final group consisted of 103 NMDC patients, 21 DCM patients and 60 HC. Analyses did not reveal any statistically significant differences in age, height, weight, BMI or sex between groups (Table 1).

None of the 60 HC had MR signs of degenerative CSC compression, whilst all 103 NMDC and 21 DCM patients had MR signs of compression varying from focal impingement to flat compressions with partially preserved or lost subarachnoid space [2,6]. The majority of patients (93.6%) had MCL at the C4/5 level and/or lower. Thus, level C3 was selected as a reference level above the compression to evaluate rostral microstructural changes.

Non-myelopathic degenerative cervical spinal cord compression patients had no radiological signs or neurological symptoms/signs of DCM. Hyperintensities on T_2-w scans were found in one cervical level in 12 DCM patients and two cervical levels in two DCM patients. The mean mJOA scale in the DCM group was 14.5.

Five out of 21 DCM patients were excluded from C3-6 analysis due to imperfect PAM50 atlas registration caused by severe compression, and these subjects were used only in the analysis of the C3 level. The accuracy of CSC segmentation and labeling was verified and corrected if necessary.

Detailed results for the relationship between dMRI metrics and compression measures are described in the Supplementary Results.

Cross-sectional area at the C3 above the compression level

The Kruskal–Wallis *H* test detected a significant between-group difference between groups in CSA above the compression level. Subsequent Dunn's post hoc tests showed significant ($p_{FWEcorr} < 0.05$) CSA reduction between HCs and NMDC patients (−5.0%, $p = 0.007$), HCs and DCM patients (−18.4%, $p < 0.0001$) and NMDC and DCM (−14.1%, $p < 0.0001$) (Table 1, Figure S1).

Correlations between dMRI metrics and demographic characteristics

Analyses revealed significant decreases ($p_{uncorr} < 0.05$) in f_1, FA, *d* and AD in the whole C3-6 area with age, whilst the opposite relationship was found between RD and age in HC (Figure S2). FA, MD, AD and *d* showed significant negative correlations with BMI (Figure S3). Correlation outcomes proved age and BMI as confounding variables, which were thus included as covariates to test between-group differences.

Distinctions between healthy controls and NMDC patients

Analysis of the C3-6 area revealed significantly ($p_{FWEcorr} < 0.05$) lower f_1 and FA in NMDC patients in dorsal and lateral tracts, that is, the fasciculus gracilis, lateral corticospinal tracts, spinal lemniscus and fasciculus cuneatus, compared to HC. Higher *d*, MD, AD and RD in NMDC patients relative to HC were observed in dorsal and lateral tracts and GM horns. Alterations in ventral columns were only revealed by the ball-and-sticks model, and NMDC patients showed higher *d* compared to HC.

TABLE 1 Characteristics of 184 participants

Characteristic	Healthy controls ($n = 60$)	NMDC patients ($n = 103$)	DCM patients ($n = 21$)	p value
Age (years)	53.7 ± 8.7	56.5 ± 9.8	58.2 ± 10.8	0.084
Sex (females/males)	38/22	59/44	12/9	0.711
Height (cm)	172.4 ± 9.8	170.0 ± 8.7	167.0 ± 10.5	0.227
Weight (kg)	78.9 ± 16.5	81.2 ± 16.7	81.7 ± 13.3	0.880
Body mass index (BMI)	26.5 ± 4.8	28.0 ± 4.6	28.8 ± 4.1	0.073
Cross-sectional area (CSA) at C3 level (mm^2)	69.7 ± 7.6	66.0 ± 7.4	56.7 ± 7.1	<0.001*
mJOA	18.0 ± 0.0	18 ± 0.0	14.5 ± 2.6	
Maximally compressed level (MCL)				
C3/4	–	5 (4.8%)	3 (14.3%)	
C4/5	–	28 (27.2%)	4 (19.0%)	
C5/6	–	49 (47.6%)	14 (66.7%)	
C6/7	–	21 (20.4%)	-	
Compression ratio (CR) at MCL	–	0.41 ± 0.07	0.35 ± 0.08	
Cross-sectional area (CSA) at MCL	–	60.71 ± 11.3	52.14 ± 13.84	
Number of stenotic levels				
1 compression	–	39 (37.9%)	6 (28.6%)	
2 compressions	–	33 (32.0%)	8 (38.1%)	
3 compressions	–	25 (24.3%)	4 (19.0%)	
4 compressions	–	6 (5.8%)	3 (14.3%)	
Electrophysiological measurements				
Abnormal MEP	–	11 patients from 87 (12.6%)	12 patients from 18 (66.7%)	
Abnormal SEP	–	28 patients from 87 (32.2%)	13 patients from 18 (72.2%)	
Abnormal EMG	–	24 patients from 92 (26.1%)	11 patients from 17 (64.7%)	

Note: Asterisk (*) indicates significance ($p < 0.05$).

Abbreviations: DCM, degenerative cervical myelopathy; EMG, electromyography; MEP, motor evoked potentials; mJOA, modified Japanese Orthopaedic Association; NMDC, non-myelopathic degenerative cervical spinal cord compression; SEP, somatosensory evoked potentials.

Lower f_1 values at C3 above the compression level were found in lateral columns, specifically in spinal lemniscus, in NMDC patients in comparison to HCs (Figures 3 and 4, Table S1).

Differences between healthy controls and DCM patients

Degenerative cervical myelopathy patients showed significantly lower f_1 and FA ($p_{FWEcorr} < 0.05$) in dorsal and lateral tracts, that is, fasciculus cuneatus, fasciculus, lateral corticospinal tracts and spinal lemniscus, in the C3-6 area compared to HC. The ball-and-sticks model demonstrated lower f_1 values in DCM patients relative to HC in ventral columns and ventral and dorsal GM horns. Higher MD and RD values in DCM patients in comparison to HC were detected in dorsal and lateral tracts, whilst higher RD in DCM patients was also observed in ventral columns. In contrast, higher d and AD in DCM patients were solely revealed in dorsal tracts. Ventral and dorsal GM horns exhibited higher d, MD, AD and RD in DCM patients compared to HC.

Lower f_1 in DCM patients relative to HC above the compression level was detected in dorsal and lateral tracts, that is, the fasciculus cuneatus, fasciculus, lateral corticospinal tracts, spinal lemniscus and dorsal GM horns, whilst lower FA affected identical areas but spared the dorsal GM. Higher MD and RD were found in dorsal and lateral columns and GM, higher d and AD were observed only in ventral GM horns and the GM of DCM patients compared to HCs. No changes were detected in dMRI metrics at the C3 level in ventral columns (Figures 3 and 4 and Table S1).

Comparisons between NMDC and DCM patients

Degenerative cervical myelopathy patients exhibited significantly lower f_1 and FA compared to NMDC patients in dorsal and lateral tracts, that is, the fasciculus cuneatus, fasciculus, lateral corticospinal

tracts and spinal lemniscus, with lower f_1 values also in the dorsal GM horns of DCM patients at the C3-6 level. Higher MD and RD were detected in the dorsal and lateral tracts as well as ventral and dorsal GM horns with higher *d* and AD in GM horns in DCM patients relative to NMDC patients.

Above the compression level, lower f_1 and FA and higher MD and RD were detected in the fasciculus cuneatus, fasciculus, lateral corticospinal tracts and spinal lemniscus, and the dorsal GM horns in DCM relative to NMDC. Higher *d* and AD were observed in GM, specifically in ventral GM horns in DCM compared to NMDC (Figures 3 and 4 and Table S1).

Relationship between dMRI and electrophysiological measures

Patients with abnormal MEP findings exhibited significantly lower f_1 and FA in lateral columns and lateral corticospinal tracts ($p_{FWEcorr} < 0.05$) and lower AD in lateral columns compared to patients with normal MEP findings in the C3-6 area. Similarly, patients with altered SEPs demonstrated significantly lower FA in the dorsal columns, fasciculus gracilis, fasciculus cuneatus and dorsal GM horns compared to unaffected patients. Abnormal EMG was also reflected by higher RD in GM and ventral GM horns comparing patients with abnormal and normal EMG (Figure 5 and Table S2).

A comparison of dMRI metrics at the C3 above the compression level revealed significantly lower f_1 and FA and higher RD in the lateral columns and lateral corticospinal tracts ($p_{FWEcorr} < 0.05$) in patients with abnormal versus normal MEP. Also, lower *d* and AD were detected in the lateral columns in patients with abnormal MEP. Altered SEP measurements were associated with lower f_1 and FA in dorsal columns, fasciculus gracilis and fasciculus cuneatus, as well as lower FA and *d* in dorsal GM horns compared to patients with normal SEP. Lower f_1, FA and RD were detected in the GM in patients with abnormal EMG compared to individuals with unaffected EMG (Figure 5 and Table S2).

Overall, patients with abnormal electrophysiological measurements showed significantly lower f_1, FA, *d* and AD values, and higher RD values, in corresponding anatomical areas in comparison to patients with normal electrophysiological findings at the compression level but also above at C3 (Figure 5 and Table S2).

Results of post hoc correlation analysis between quantitative electrophysiological parameters and dMRI metrics are shown in the Supplementary Results.

Relationship between dMRI and clinical mJOA scale at the C3 level in DCM

Exploratory correlation analysis revealed significant positive correlations between mJOA and f_1, FA, *d* and AD from the C3 level in lateral columns in DCM patients. FA, AD and *d* in the spinal lemniscus and FA in ventral columns showed significant positive correlations with the mJOA scale. A negative relationship was identified between the mJOA scale and RD in lateral columns (Figures 6 and S6).

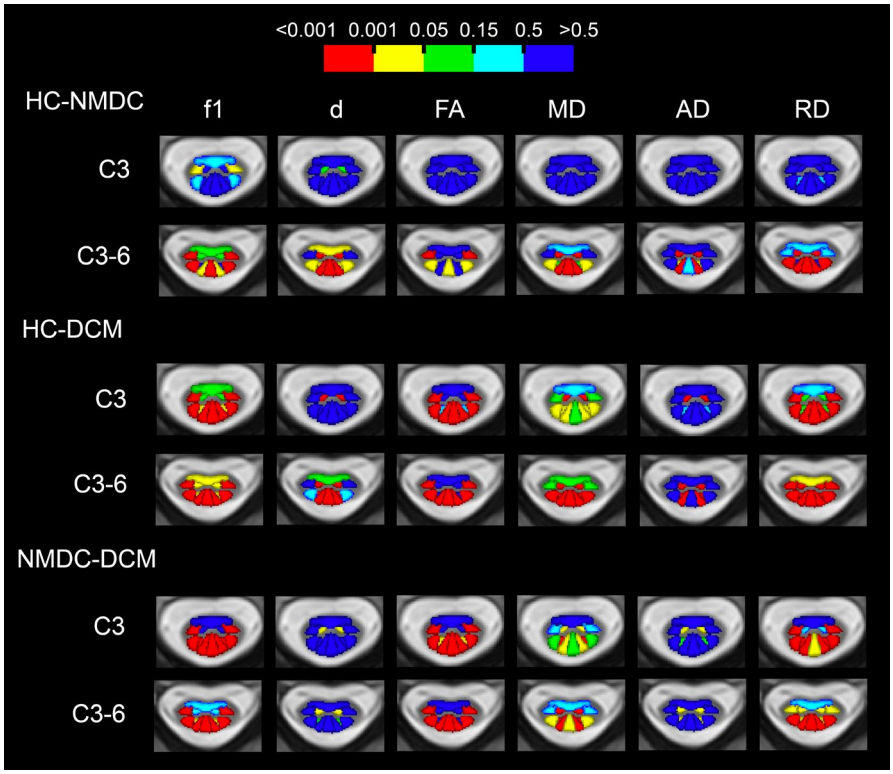

FIGURE 3 Between-group differences in diffusion metrics for tract-specific ROIs from C3 above the compression level and C3-6 area color coded by their *p* values ($p_{FWEcor} < 0.05$)

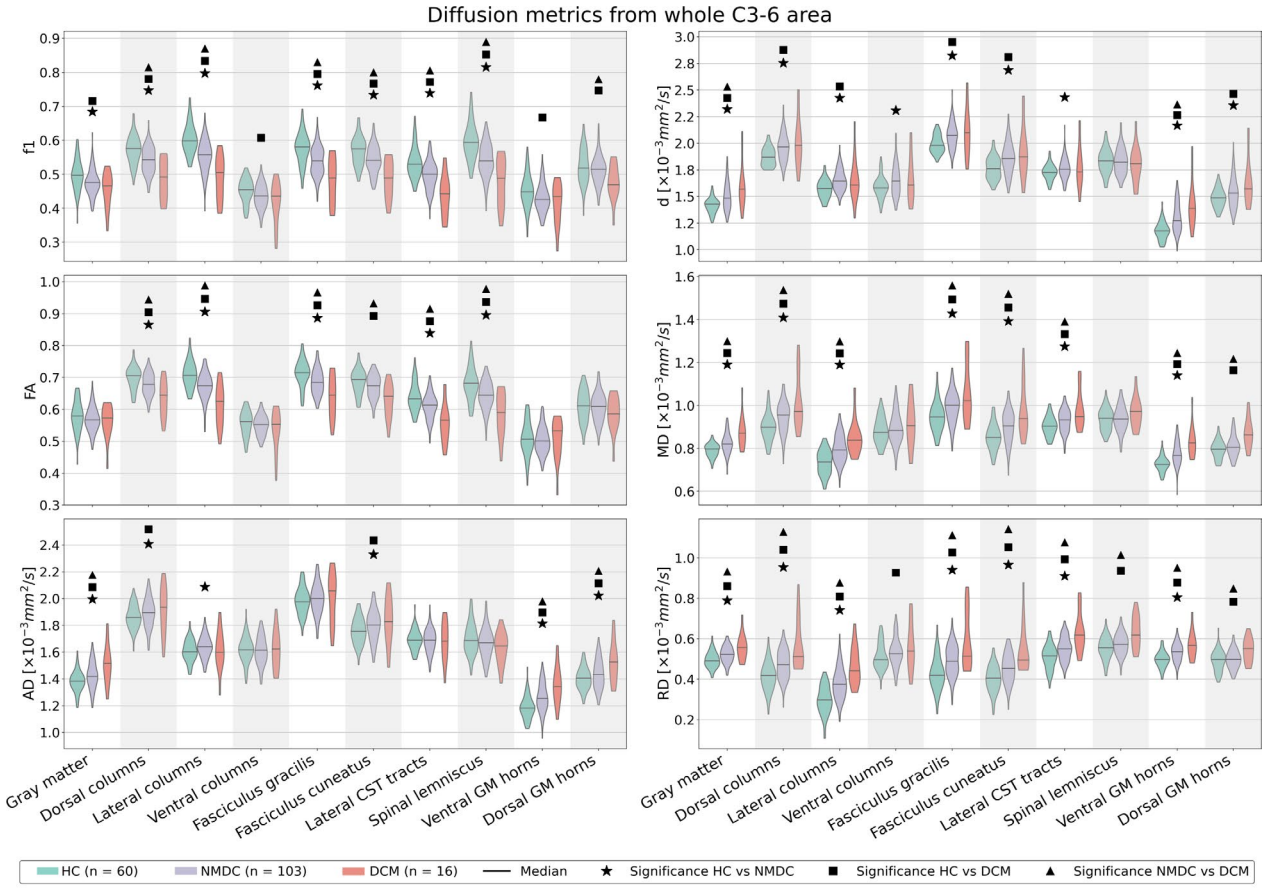

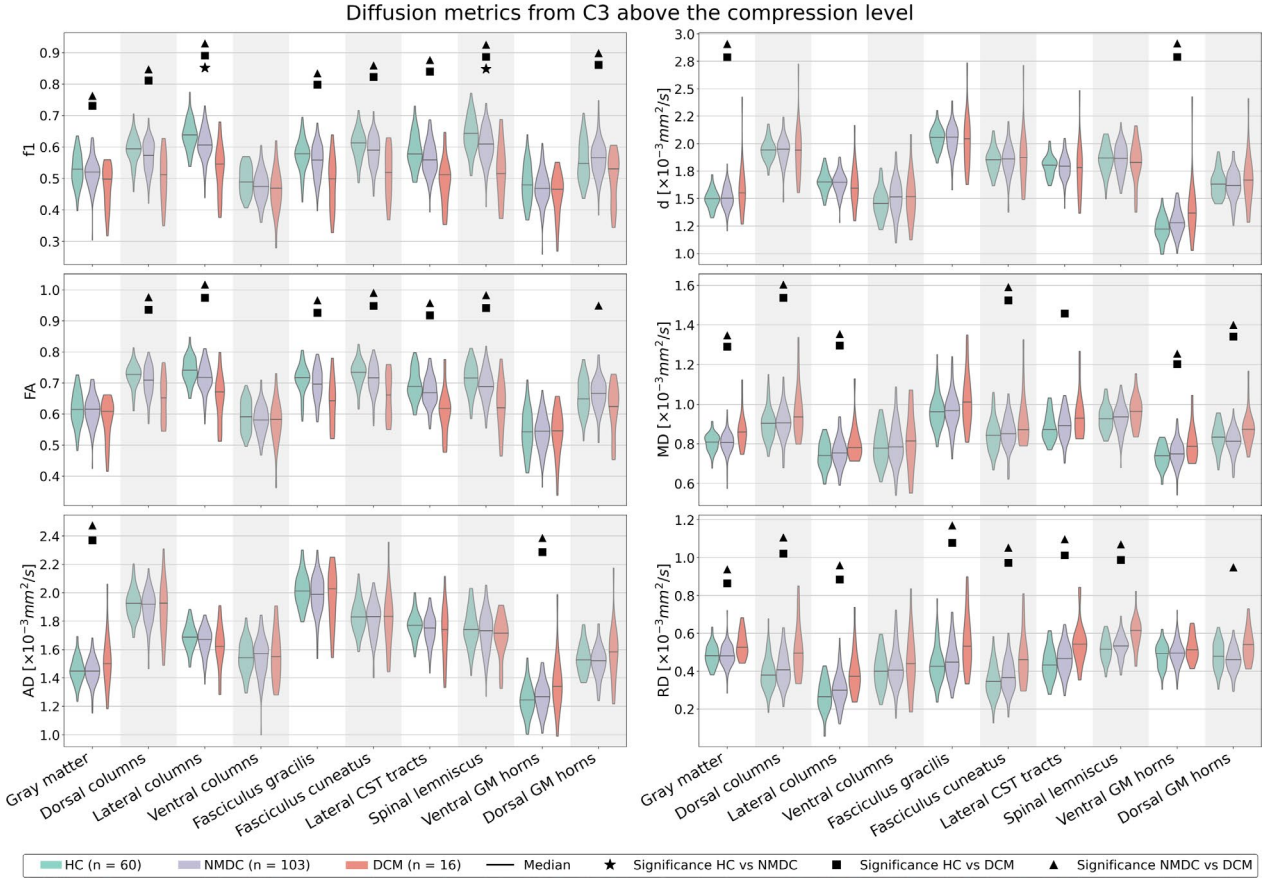

FIGURE 4 Violin plots showing between-group differences from the C3-6 area and C3 above the compression level. Markers indicate $p_{\text{FWEcorr}} < 0.05$

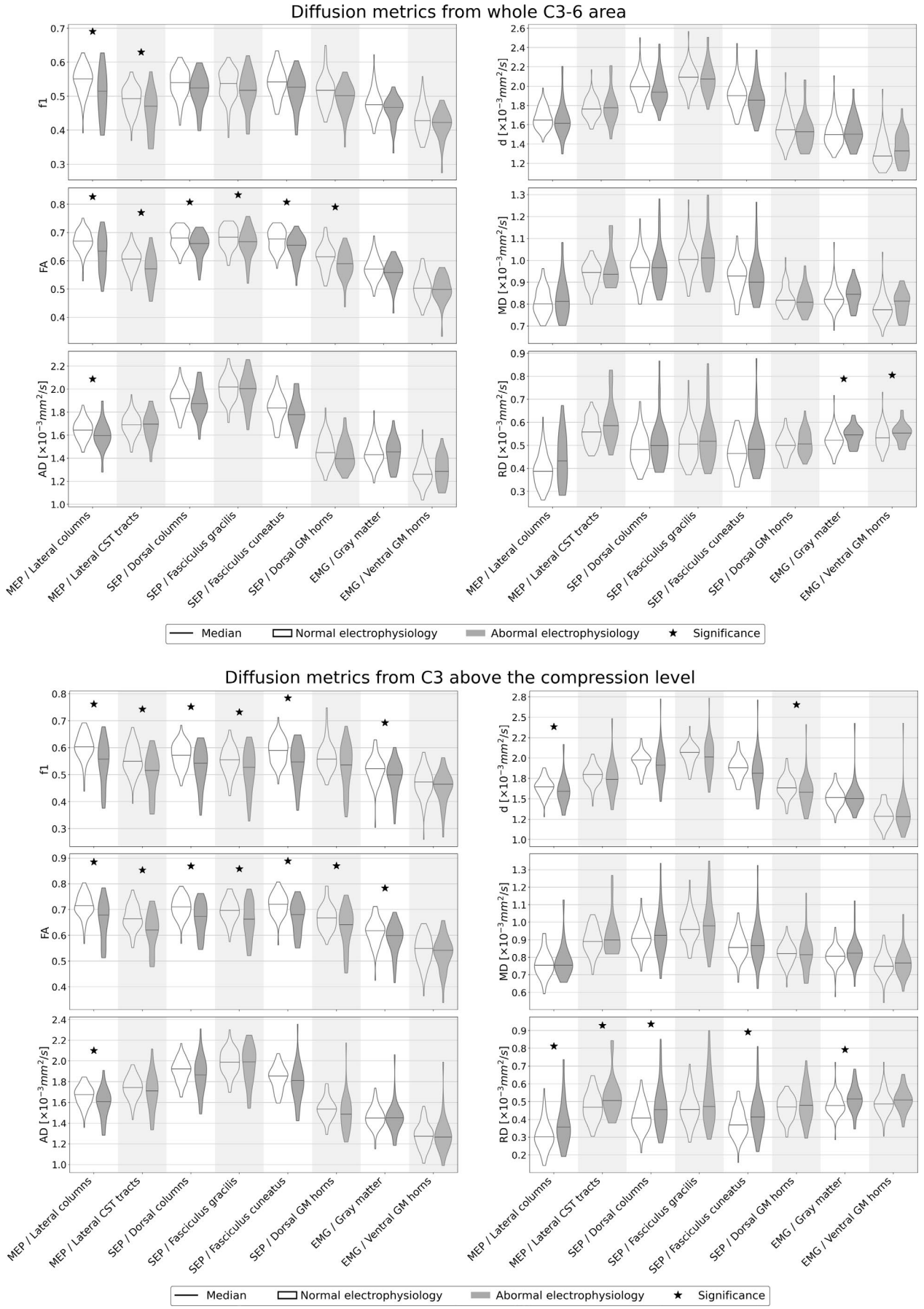

FIGURE 5 Violin plots showing relationship between electrophysiological finding and diffusion metrics extracted from the C3-6 area and C3 above the compression level. Asterisks (*) indicate $p_{\text{FWEcorr}} < 0.05$

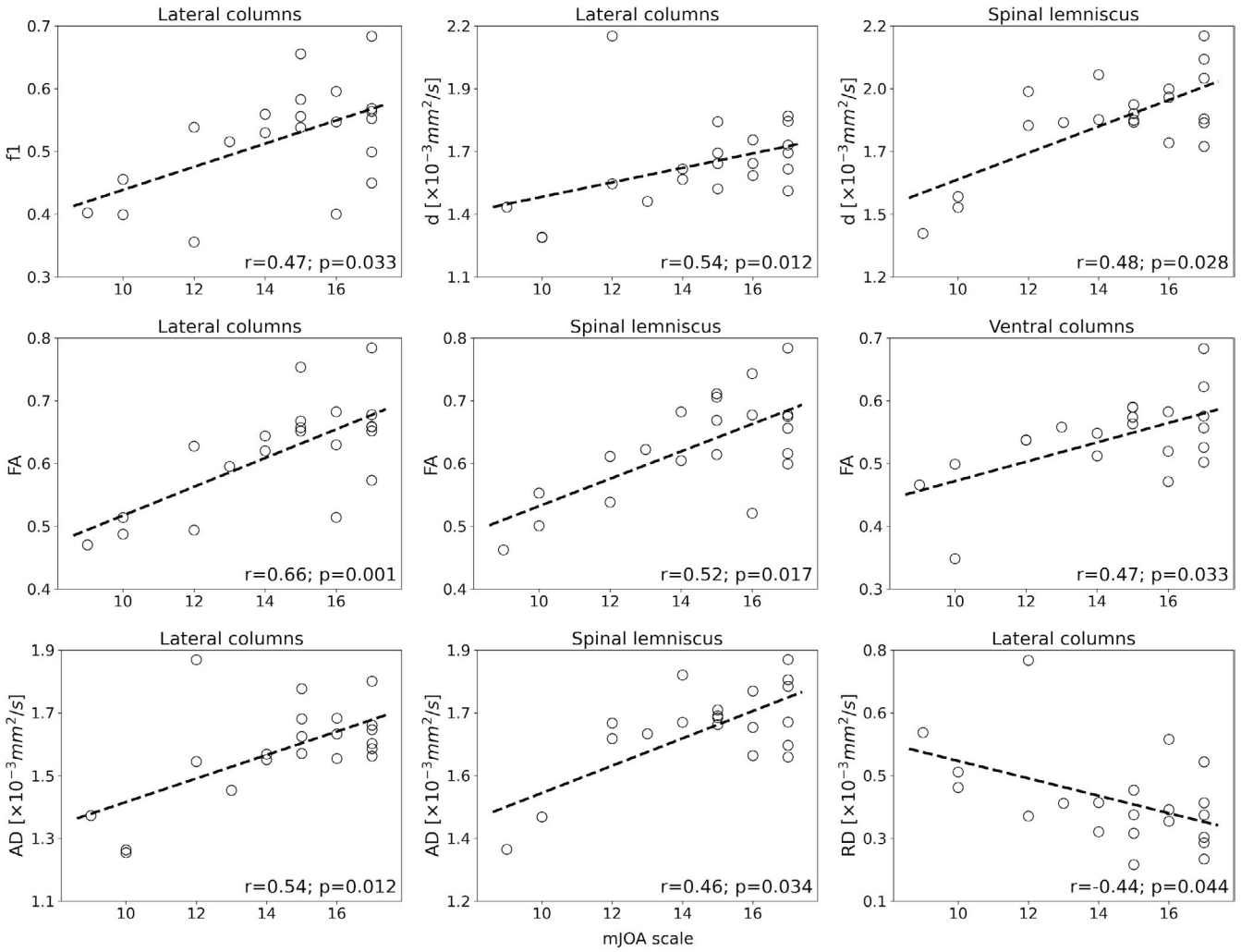

FIGURE 6 Correlations between dMRI metrics from C3 above the compression level and the modified Japanese Orthopaedic Association (mJOA) scale in DCM patients

DISCUSSION

Our study detected tract-specific distinctions in diffusion metrics between NMDC and symptomatic DCM patients compared to HC in the GM and dorsal columns, that is, fasciculus gracilis, fasciculus cuneatus, and in the lateral columns composed of lateral corticospinal tracts and spinal lemniscus. DCM patients also showed additional alterations in the ventral columns compared to HC. Diffusion changes were found in the C3-6 area as well as above the compression level at C3, and were accompanied by reduced cord cross-sectional area at the C3 level in both NMDC and DCM relative to HC. Importantly, diffusion metrics in the GM and motor and sensory tracts correlated with relevant electrophysiological abnormalities and clinical mJOA scale, implying the critical importance of tract-specific measures for future longitudinal studies.

Differences in dMRI metrics in the C3-6 area in NMDC patients compared to HC confirmed incipient CSC damage in the early stages of degenerative compression in the dorsal and lateral tracts. The findings align with post-mortem histopathological studies, in which chronic CSC compression led to damage of the lateral pial plexus resulting in limited blood flow and axonal degeneration of lateral corticospinal tracts and dorsal areas [1]. Malperfusion through the compressed anterior spinal artery initially affects GM, lateral columns and the anterior part of the dorsal columns and can ultimately result in progressive demyelination [1,27]. Indeed, lower f_1 and FA and higher diffusivity metrics in the lateral and dorsal tracts and GM observed in our study in NMDC and DCM patients compared to HC suggest ongoing demyelination [13]. Differences in f_1 in the lateral and dorsal tracts separated DCM from NMDC with more profound deficits found in DCM than NMDC patients. Thus, dMRI alterations corroborate post-mortem studies, which reported lesions of the anterior GM horns, the lateral tracts and the anterior part of the dorsal tracts but showed no changes in the ventral columns in the early stages of degenerative compression [13,33]. Additional f_1 and RD deficits occur in ventral columns as the compression progresses from NMDC to symptomatic DCM. Our findings thus align with histopathological samples when revealing alterations in diffusion metrics in ventral columns in DCM but not in NMDC. Direct comparison between NMDC and DCM groups showed profound changes in dorsal and lateral columns as well as GM that further confirmed the influence of gradual alteration

of arterial flow on the compression-related deficits and myelopathy [34,35]. Whilst lower FA corroborates previous DTI studies in DCM patients [10,14,36-38], asymptomatic patients with CSC compression [16] and patients with slowly progressing CSC compression [39], to date no study showed tract-specific changes in a large sample of both NMDC and DCM patients. Spatial distinctions in alterations between DCM and NMDC further emphasize the necessity of tract-specific analysis in CSC studies.

Our findings also demonstrate malicious effects of the compression on microstructural CSC integrity above the compression level at the C3 level. Deficits at C3 in NMDC were limited to the spinal lemniscus and were depicted solely using the ball-and-sticks f_1 metric pointing to incipient remote degeneration in NMDC patients in the early stages of degenerative CSC compression. As the compression progressed to DCM, additional f_1, FA and RD alterations in dorsal and lateral columns occurred. The ball-and-sticks f_1 demonstrated higher discrimination when showing changes in the spinal lemniscus that were not detected using the DTI model. Significantly lower f_1 and FA above the compression level in DCM patients compared to HC point to progressive anterograde and retrograde axonal degeneration of dorsal sensory pathways such as fasciculus gracilis, cuneatus and spinal lemniscus as well as lateral motor corticospinal tracts, respectively [1,13,14]. Alterations of FA at the C3 level are in agreement with a recent study from Seif et al. [14] which demonstrated a remote FA decrease in the lateral corticospinal and spinothalamic tracts at the C2/3 level in DCM patients and patients with traumatic spinal cord injury compared to HC. Changes in GM along with spinal cord CSA reduction above the compression level in DCM patients compared to NMDC patients and HC point to trans-synaptic degeneration and GM atrophy above the stenosis level in patients with myelopathy [13]. Direct comparison between symptomatic DCM and NMDC patients demonstrated more severe deficits in DCM patients in the dorsal and lateral columns, as well as in the ventral and dorsal GM horns. Whereas remote degeneration in DCM patients compared to HC corroborates previous reports [13,14,38,40,41], tract-based approaches also delineated gradual changes between NMDC and symptomatic DCM patients. Alterations above the compression level further endorse brain studies [42-44] that reported changes in motor and somatosensory cortex in symptomatic DCM patients with degenerative CSC compression. A decrease of CSA at the C3 level in DCM compared to HC corresponds with previous studies [10,13,14,40] and further points to remote degeneration rostrally to MCL. A smaller yet significant CSA deficit was also found in the NMDC group, suggesting more profound changes in DCM than in NMDC compared to HC.

Tract-specific analysis also revealed a relationship between the degree of disability (i.e., mJOA scale) and diffusion metrics in lateral columns and spinal lemniscus comprising motor and sensory pathways in DCM patients. DCM patients with lower mJOA scale (worse DCM disability) exhibited a decrease of f_1, FA and AD and an increase of RD compared to NMDC patients and HC. These findings correspond to more severe demyelination and axonal damage in DCM patients with profound motor and sensory disability.

Most importantly, significant dMRI changes in individual tracts between patients with and without electrophysiological deficits point to a crucial relationship between functional impairments and microstructural dMRI degeneration. Patients with abnormal electrophysiology findings showed lower values of f_1, FA, d and AD metrics and higher values of RD and MD compared to those with normal electrophysiological findings. Microstructural changes in sensory and motor tracts were related to SEP and MEP, respectively, with altered GM found in patients with EMG changes. Whilst previous studies also examined the relationship between dMRI and electrophysiology, they failed to detect dMRI distinctions between patients with and without electrophysiological deficits [18], or detected FA alterations in DCM patients with normal SEP [38]. Whereas electrophysiological measures serve as essential predictors of DCM development [2,6], optimized spatially selective tract-based measures of the CSC overcome previous unselective dMRI analyses of the whole axial spinal cord volumes. Thus, the proven significant relationship between electrophysiology and tract-based dMRI metrics suggest that tract-specific analysis might provide an objective tool to examine the relationship between diffusion-informed microstructural changes and functional electrophysiological impairments. Tract-specific dMRI should be explored as a potential predictor in future longitudinal studies utilizing current high-resolution methods. Also, dMRI is a non-invasive tool that is easier to perform than electrophysiological measures.

Our outcomes imply the importance of novel dMRI models in CSC analysis. The multi-compartment ball-and-sticks model, which incorporates intra-axonal restriction and better explains the data than DTI [20], has not been utilized in a large sample of NMDC or DCM patients yet. The ball-and-sticks f_1 metric indeed revealed additional between-group alterations at the C3-*6* area in GM as well as ventral columns and fasciculus cuneatus, which were not revealed by FA. Lemniscal alterations between NMDC patients and HCs at C3 above the compression level were also exclusively revealed by the ball-and-sticks f_1 metric.

Our study was limited by spatial coverage of dMRI data (i.e., the C3-6 area). Caudal vertebral levels were not explored due to scanning time constraints and possible signal loss at the C7 level caused by the character of the HARDI-ZOOMit protocol [21]. Semi-automatic analyses also required time-consuming manual adjustment of segmentations, mainly in patients with severe CSC compression. Severe compression further limited proper white matter atlas registration in five DCM patients. Although the atlas-based approach provides higher accuracy and less propensity to susceptibility distortions than tractography-based methods [45], future studies may benefit from subject-specific tractography approaches, which are not yet fully developed.

In conclusion, the combination of conventional DTI and the multi-compartment ball-and-sticks model allowed to reveal tract-specific dMRI changes congruent with previous histopathological studies. Compression-caused demyelination, atrophy and axonal degeneration in white matter tracts and GM progressed from less severe NMDC to symptomatic DCM. Tract-specific diffusion abnormalities

correlated with clinical deficits and abnormal electrophysiology in relevant anatomical tracts. Thus, our study demonstrated that high-resolution tract-specific dMRI is a sensitive microstructural marker of CSC alterations for longitudinal trials aiming to provide early predictors of progression into symptomatic myelopathy and potentially can be translated also for patients with traumatic spinal cord injury.

ACKNOWLEDGEMENTS

The authors would like to thank to Pavel Hok for help with data processing, Petr Kudlička and Veronika Fábíková for MRI data acquisition and Dagmar Kratochvílová for subject recruitment.

CONFLICT OF INTEREST

No authors disclosed any relevant relationships.

AUTHOR CONTRIBUTIONS

Jan Valošek: Conceptualization (equal); data curation (equal); formal analysis (equal); funding acquisition (supporting); investigation (equal); methodology (equal); resources (supporting); software (equal); validation (equal); visualization (lead); writing—original draft (lead); writing—review and editing (lead). René Labounek: Conceptualization (equal); data curation (equal); formal analysis (equal); funding acquisition (equal); investigation (equal); methodology (equal); resources (equal); software (equal); supervision (equal); validation (equal); visualization (equal); writing—original draft (equal); writing—review and editing (equal). Tomáš Horák: Data curation (equal); formal analysis (equal); investigation (equal); methodology (equal); software (equal); validation (equal); visualization (equal); writing—original draft (equal); writing—review and editing (equal). Magda Horakova: Data curation (equal); investigation (equal); methodology (equal); project administration (equal); software (equal); validation (equal); visualization (equal); writing—original draft (equal); writing—review and editing (equal). Petr Bednařík: Conceptualization (equal); data curation (equal); formal analysis (equal); funding acquisition (equal); investigation (equal); methodology (equal); resources (equal); software (equal); supervision (equal); validation (equal); visualization (equal); writing—original draft (equal); writing—review and editing (equal). Miloš Keřkovský: Conceptualization (equal); data curation (equal); formal analysis (equal); funding acquisition (equal); investigation (equal); methodology (equal); project administration (equal); resources (equal); software (equal); supervision (equal); validation (equal); writing—original draft (equal); writing—review and editing (equal). Jan Kočica: Data curation (equal); investigation (equal); validation (equal); visualization (equal); writing—original draft (equal); writing—review and editing (equal). Tomáš Rohan: Data curation (equal); investigation (equal); validation (equal); visualization (equal); writing—original draft (equal); writing—review and editing (equal). Christophe Lenglet: Conceptualization (equal); investigation (equal); methodology (equal); supervision (equal); visualization (equal); writing—original draft (equal); writing—review and editing (equal). Julien Cohen-Adad: Data curation (equal); investigation (equal); methodology (equal); supervision (equal); validation (equal); visualization (equal); writing—original draft (equal); writing—review and editing (equal). Petr Hlustik: Conceptualization (equal); data curation (equal); formal analysis (equal); funding acquisition (equal); investigation (equal); methodology (equal); project administration (equal); resources (equal); software (equal); supervision (lead); validation (equal); visualization (equal); writing—original draft (equal); writing—review and editing (equal). Eva Vlckova: Conceptualization (equal); data curation (equal); formal analysis (equal); funding acquisition (equal); investigation (equal); methodology (equal); project administration (equal); validation (equal); visualization (equal); writing—original draft (equal); writing—review and editing (equal). Zdeněk Kadaňka Jr: Conceptualization (equal); investigation (equal); methodology (equal); validation (equal); visualization (equal); writing—original draft (equal); writing—review and editing (equal). Josef Bednarik: Conceptualization (lead); data curation (equal); formal analysis (equal); funding acquisition (lead); investigation (equal); methodology (equal); project administration (lead); resources (lead); software (equal); supervision (lead); validation (equal); visualization (equal); writing—original draft (equal); writing—review and editing (equal). Alena Svatkova: Conceptualization (equal); data curation (equal); formal analysis (equal); funding acquisition (equal); investigation (equal); methodology (equal); resources (equal); software (equal); supervision (lead); validation (equal); visualization (equal); writing—original draft (equal); writing—review and editing (equal).

DATA AVAILABILITY STATEMENT

The data that support the findings of this study are available from the corresponding author upon reasonable request.

ORCID

Jan Valošek https://orcid.org/0000-0002-7398-4990
René Labounek https://orcid.org/0000-0003-0439-1304
Tomáš Horák https://orcid.org/0000-0003-1743-1133
Magda Horáková https://orcid.org/0000-0003-3317-2661
Petr Bednařík https://orcid.org/0000-0002-8828-7661
Miloš Keřkovský https://orcid.org/0000-0003-0587-9897
Jan Kočica https://orcid.org/0000-0002-2937-6373
Tomáš Rohan https://orcid.org/0000-0002-7105-583X
Christophe Lenglet https://orcid.org/0000-0003-4646-3185
Julien Cohen-Adad https://orcid.org/0000-0003-3662-9532
Petr Hluštík https://orcid.org/0000-0002-1951-0671
Eva Vlčková https://orcid.org/0000-0003-2322-5539
Zdeněk Kadaňka Jr. https://orcid.org/0000-0001-5146-2457
Josef Bednařík https://orcid.org/0000-0001-7420-2383
Alena Svatkova https://orcid.org/0000-0002-9188-4280

REFERENCES

1. Badhiwala JH, Ahuja CS, Akbar MA, et al. Degenerative cervical myelopathy—update and future directions. *Nat Rev Neurol*. 2020;16:108-124.
2. Bednarik J, Kadanka Z, Dusek L, et al. Presymptomatic spondylotic cervical myelopathy: an updated predictive model. *Eur Spine J*. 2008;17:421-431.
3. Smith SS, Stewart ME, Davies BM, et al. The prevalence of asymptomatic and symptomatic spinal cord compression on magnetic

resonance imaging: a systematic review and meta-analysis. *Global Spine Journal*. 2021;11(4):597-607.
4. Kovalova I, Kerkovsky M, Kadanka Z, et al. Prevalence and imaging characteristics of nonmyelopathic and myelopathic spondylotic cervical cord compression. *Spine (Phila Pa 1976)*. 2016;41(24):1908-1916.
5. Adamova B, Bednarik J, Andrasinova T, et al. Does lumbar spinal stenosis increase the risk of spondylotic cervical spinal cord compression? *Eur Spine J*. 2015;24:2946-2953.
6. Kadanka Z, Adamova B, Kerkovsky M, et al. Predictors of symptomatic myelopathy in degenerative cervical spinal cord compression. *Brain Behav*. 2017;7:e00797.
7. Bednarik J, Kadanka Z, Dusek L, et al. Presymptomatic spondylotic cervical cord compression. *Spine (Phila Pa 1976)*. 2004;29(20):2260-2269.
8. Witiw CD, Mathieu F, Nouri A, et al. Clinico-radiographic discordance: an evidence-based commentary on the management of degenerative cervical spinal cord compression in the absence of symptoms or with only mild symptoms of myelopathy. *Glob Spine J*. 2018;8:527-534.
9. Wilson JR, Barry S, Fischer DJ, et al. Frequency, timing, and predictors of neurological dysfunction in the nonmyelopathic patient with cervical spinal cord compression, canal stenosis, and/or ossification of the posterior longitudinal ligament. *Spine (Phila Pa 1976)*. 2013;38:S37-S54.
10. Martin AR, De Leener B, Cohen-Adad J, et al. A novel MRI biomarker of spinal cord white matter injury: T2*-weighted white matter to gray matter signal intensity ratio. *Am J Neuroradiol*. 2017;38:1266-1273.
11. Dong F, Wu Y, Song P, et al. A preliminary study of 3.0-T magnetic resonance diffusion tensor imaging in cervical spondylotic myelopathy. *Eur Spine J*. 2018;27:1839-1845.
12. Shabani S, Kaushal M, Budde MD, et al. Diffusion tensor imaging in cervical spondylotic myelopathy: a review. *J Neurosurg Spine*. 2020;33:65-72.
13. David G, Mohammadi S, Martin AR, et al. Traumatic and nontraumatic spinal cord injury: pathological insights from neuroimaging. *Nat Rev Neurol*. 2019;15:718-731.
14. Seif M, David G, Huber E, et al. Cervical cord neurodegeneration in traumatic and non-traumatic spinal cord injury. *J Neurotrauma*. 2020;37:860-867.
15. Martin AR, De Leener B, Cohen-Adad J, et al. Monitoring for myelopathic progression with multiparametric quantitative MRI. *PLoS One*. 2018;13(4):e0195733.
16. Martin AR, De Leener B, Cohen-Adad J, et al. Can microstructural MRI detect subclinical tissue injury in subjects with asymptomatic cervical spinal cord compression? A prospective cohort study. *BMJ Open*. 2018;8:e019809.
17. Keřkovský M, Bednařík J, Jurová B, et al. Spinal cord MR diffusion properties in patients with degenerative cervical cord compression. *J Neuroimaging*. 2017;27:149-157.
18. Kerkovský M, Bednarík J, Dušek L, et al. Magnetic resonance diffusion tensor imaging in patients with cervical spondylotic spinal cord compression: correlations between clinical and electrophysiological findings. *Spine (Phila Pa 1976)*. 2012;37(1):48-56.
19. Basser PJ, Mattiello J, LeBihan D. MR diffusion tensor spectroscopy and imaging. *Biophys J*. 1994;66:259-267.
20. Panagiotaki E, Schneider T, Siow B, et al. Compartment models of the diffusion MR signal in brain white matter: a taxonomy and comparison. *NeuroImage*. 2012;59:2241-2254.
21. Labounek R, Valošek J, Horák T, et al. HARDI-ZOOMit protocol improves specificity to microstructural changes in presymptomatic myelopathy. *Sci Rep*. 2020;10:17529.
22. Behrens TEJ, Woolrich MW, Jenkinson M, et al. Characterization and propagation of uncertainty in diffusion-weighted MR imaging. *Magn Reson Med*. 2003;50:1077-1088.
23. Gros C, De Leener B, Badji A, et al. Automatic segmentation of the spinal cord and intramedullary multiple sclerosis lesions with convolutional neural networks. *NeuroImage*. 2019;184:901-915.
24. De Leener B, Fonov VS, Collins DL, Callot V, Stikov N, Cohen-Adad J. PAM50: unbiased multimodal template of the brainstem and spinal cord aligned with the ICBM152 space. *NeuroImage*. 2018;165:170-179.
25. Lévy S, Benhamou M, Naaman C, et al. White matter atlas of the human spinal cord with estimation of partial volume effect. *NeuroImage*. 2015;119:262-271.
26. De Leener B, Lévy S, Dupont SM, et al. SCT: Spinal Cord Toolbox, an open-source software for processing spinal cord MRI data. *NeuroImage*. 2017;145:24-43.
27. Mair WGP, Druckman R. The pathology of spinal cord lesions and their relation to the clinical features in protrusion of cervical intervertebral discs (a report of four cases). *Brain*. 1953;76:70-91.
28. Tetreault L, Kopjar B, Nouri A, et al. The modified Japanese Orthopaedic Association scale: establishing criteria for mild, moderate and severe impairment in patients with degenerative cervical myelopathy. *Eur Spine J*. 2017;26:78-84.
29. Bednařík J, Kadaňka Z, Voháňka S, et al. The value of somatosensory and motor evoked potentials in pre-clinical spondylotic cervical cord compression. *Eur Spine J*. 1998;7:493-500.
30. Caruyer E, Lenglet C, Sapiro G, et al. Design of multishell sampling schemes with uniform coverage in diffusion MRI. *Magn Reson Med*. 2013;69:1534-1540.
31. Jenkinson M, Beckmann CF, Behrens TEJ, et al. FSL. *NeuroImage*. 2012;62:782-790.
32. Ullmann E, Pelletier Paquette JF, Thong WE, et al. Automatic labeling of vertebral levels using a robust template-based approach. *Int J Biomed Imaging*. 2014;2014:719520.
33. Cohen-Adad J. Microstructural imaging in the spinal cord and validation strategies. *NeuroImage*. 2018;182:169-183.
34. Badhiwala JH, Ahuja CS, Akbar MA, et al. Degenerative cervical myelopathy - update and future directions. *Nat Rev Neurol*. 2020;16(2):108-124.
35. Baptiste DC, Fehlings MG. Pathophysiology of cervical myelopathy. *Spine J*. 2006;6(6 Suppl):190S-197S.
36. Lee JW, Kim JH, Park JB, et al. Diffusion tensor imaging and fiber tractography in cervical compressive myelopathy: preliminary results. *Skeletal Radiol*. 2011;40:1543-1551.
37. Lindberg PG, Sanchez K, Ozcan F, et al. Correlation of force control with regional spinal DTI in patients with cervical spondylosis without signs of spinal cord injury on conventional MRI. *Eur Radiol*. 2016;26:733-742.
38. Wen CY, Cui JL, Liu HS, et al. Is diffusion anisotropy a biomarker for disease severity and surgical prognosis of cervical spondylotic myelopathy. *Radiology*. 2014;270:197-204.
39. Facon D, Ozanne A, Fillard P, et al. MR diffusion tensor imaging and fiber tracking in spinal cord compression. *AJNR Am J Neuroradiol*. 2005;26:1587-1594.
40. Grabher P, Mohammadi S, Trachsler A, et al. Voxel-based analysis of grey and white matter degeneration in cervical spondylotic myelopathy. *Sci Rep*. 2016;6:24636.
41. Budzik J-F, Balbi V, Le Thuc V, Duhamel A, Assaker R, Cotten A. Diffusion tensor imaging and fibre tracking in cervical spondylotic myelopathy. *Eur Radiol*. 2011;21:426-433.
42. Kowalczyk I, Duggal N, Bartha R. Proton magnetic resonance spectroscopy of the motor cortex in cervical myelopathy. *Brain*. 2012;135:461-468.
43. Bernabéu-Sanz Á, Mollá-Torró JV, López-Celada S, et al. MRI evidence of brain atrophy, white matter damage, and functional adaptive changes in patients with cervical spondylosis and prolonged spinal cord compression. *Eur Radiol*. 2020;30:357-369.
44. Zhou FQ, Tan YM, Wu L, Zhuang Y, He LC, Gong HH. Intrinsic functional plasticity of the sensory-motor network in patients with cervical spondylotic myelopathy. *Sci Rep*. 2015;5(1):9975.

45. Cohen-Adad J, Wheeler-Kingshott C. *Quantitative MRI of the Spinal Cord*. San Diego, CA: Academic Press (Elsevier); 2014.

SUPPORTING INFORMATION

Additional supporting information may be found online in the Supporting Information section.

Supplementary Material

How to cite this article: Valošek J, Labounek R, Horák T, et al. Diffusion magnetic resonance imaging reveals tract-specific microstructural correlates of electrophysiological impairments in non-myelopathic and myelopathic spinal cord compression. *Eur J Neurol*. 2021;28:3784–3797. https://doi.org/10.1111/ene.15027